

Proposal of a cold-atom realization of quantum maps with Hofstadter's butterfly spectrum

Jiao Wang¹ and Jiangbin Gong^{2,3,*}

¹*Temasek Laboratories and Beijing-Hong Kong-Singapore Joint Centre for Nonlinear and Complex Systems (Singapore), National University of Singapore, 117542, Singapore*

²*Department of Physics and Centre of Computational Science and Engineering, National University of Singapore, 117542, Singapore*

³*NUS Graduate School for Integrative Sciences and Engineering, Singapore 117597, Republic of Singapore*

(Received 4 October 2007; published 27 March 2008)

Quantum systems with Hofstadter's butterfly spectrum are of fundamental interest to many research areas. Based upon slight modifications of existing cold-atom experiments, a cold-atom realization of quantum maps with Hofstadter's butterfly spectrum is proposed. Connections and differences between our realization and the kicked Harper model are identified. This work also exposes, for the first time, a simple connection between the kicked Harper model and the kicked rotor model, the two paradigms of classical and quantum chaos.

DOI: [10.1103/PhysRevA.77.031405](https://doi.org/10.1103/PhysRevA.77.031405)

PACS number(s): 37.10.De, 05.45.Mt, 03.65.-w, 05.60.Gg

The Harper model [1] plays a fundamental role in many research areas because it yields the famous Hofstadter's butterfly spectrum [2,3]. This fractal spectrum, first discovered in two-dimensional electron systems subject to a square lattice potential and a perpendicular magnetic field [2], has found applications in studies of quantum Hall effect [4,5], the renormalization group [6], high-temperature superconductivity [7], to name a few. Various effects on Hofstadter's butterfly spectrum were carefully examined [8]. Systems with a butterfly spectrum should also be of general interest to quantum phase transition studies because it implies an infinite number of phases when some external parameters are scanned. Systems with Hofstadter's butterfly spectrum were also studied experimentally [4,9].

Hofstadter's butterfly can emerge in the quasienergy spectrum of periodically driven systems as well. In this context, the kicked Harper model (KHM), adapted from the Harper model by considering a delta-kicking potential, has attracted vast interests [10]. The Hamiltonian of the KHM is given by $H_{\text{KHM}} = (L/T)\cos(p) + K\cos(q)\sum_n \delta(t-nT)$, where L and K are two system parameters, T is the kicking period, p and q ($q \in [0, 2\pi]$) are conjugate momentum and angle variables, with their commutation relation defining the effective Planck constant \hbar , namely, $[q, p] = i\hbar$. The Hilbert space with the periodic boundary condition in q is spanned by the eigenfunctions $|m\rangle$ of p , with $p|m\rangle = m\hbar|m\rangle$, $\langle q|m\rangle = \exp(imq)/\sqrt{2\pi}$, and m being an integer. The KHM quantum map associated with the unitary evolution for each period T is given by

$$U_{\text{KHM}} = e^{-i(L/\hbar)\cos(p)} e^{-i(K/\hbar)\cos(q)}. \quad (1)$$

Because the classical limit of the quantum map U_{KHM} is chaotic in general, this map has become a paradigm for understanding (i) how a fractal quasienergy spectrum affects the quantum dynamics and the associated quantum-classical correspondence, and (ii) how the underlying classical chaos affects the butterfly. For experimental realizations of the KHM, one early study proposed to use Fermi-surface elec-

trons in external fields [11]. Another study showed that the system of a charged particle kicked by a designed field sequence [12] can be mapped onto the KHM. However, these two proposals have not led to experiments. Connections between the KHM and the so-called kicked harmonic oscillator model were also noticed [13], but only for the special case of $K=L$.

Using cold atoms periodically kicked by an optical lattice, about ten laboratories worldwide [14–17] have realized the so-called kicked-rotor model (KRM) [18] as another quantum map paradigm. Using similar notation as above and in the same Hilbert space as the KHM, the Hamiltonian of the KRM is given by $H_{\text{KRM}} = p^2/2 + K\cos(q)\sum_n \delta(t-nT)$. Many variants of the KRM, obtained by considering different types of kicking sequences or additional external potentials, have also been achieved. In these studies the experimental setup itself has also advanced, from using thermal atoms to using a Bose-Einstein condensate (BEC) [15,16] that has very large coherence width. These ongoing experimental efforts motivate the following bold and important question: can these cold-atom laboratories working on the KRM also realize the kicked Harper model or its variants by slightly modifying their existing apparatus? If yes, quantum maps with Hofstadter's butterfly spectrum can soon be experimentally realized in many cold-atom laboratories, an entirely new generation of experiments can be planned, and novel applications of cold-atom researches may be established.

Stimulated by our early work seeking a potential connection between KHM and a variant of KRM [19], a very positive answer to the above question is indeed provided here. In particular, we show that previous experimental setup for the so-called double-kicked rotor model (DKRM) [17,20] already suffices for synthesizing a quantum map displaying Hofstadter's butterfly, provided that one quantum resonance condition therein is met and the initial atom cloud is a BEC that has sufficient coherence width. The butterfly spectrum associated with the obtained quantum map is almost indistinguishable from the standard result previously calculated for the KHM. We then show connections and dramatic dynamical differences between our quantum map and the KHM. In addition to experimental interests, the results should also motivate more theoretical work on quantum maps with Hofstadter's butterfly spectrum.

*phygj@nus.edu.sg

Consider then a DKRM that is already experimentally realized [17]. Using the same notation as above, the Hamiltonian of a DKRM can be written as $H_{\text{DKRM}} = p^2/2 + K_1 \cos(q) \sum_n \delta(t - nT) + K_2 \cos(q) \sum_n \delta(t - nT - \eta)$. Evidently, in addition to kicks at $t = nT$, the rotor in a DKRM is also subject to kicks at $t = nT + \eta$. The associated quantum map U_{DKRM} for a period from $nT + 0^-$ to $(n+1)T + 0^-$ is given by

$$U_{\text{DKRM}} = e^{-i(T-\eta)(p^2/2\hbar)} e^{-i(K_2/\hbar)\cos(q)} e^{-i\eta(p^2/2\hbar)} e^{-i(K_1/\hbar)\cos(q)}. \quad (2)$$

Remarkably, if we now require the parameter T to satisfy the quantum resonance condition of the KRM, i.e., $T\hbar = 4\pi$, then due to the discreteness of the momentum eigenvalues, one obtains $e^{-iT(p^2/2\hbar)} = 1$ when operating on any state in the Hilbert space defined above. Under this resonance condition we are able to reduce U_{DKRM} to U_{DKRM}^r ,

$$U_{\text{DKRM}}^r = e^{i\eta(p^2/2\hbar)} e^{-i(K_2/\hbar)\cos(q)} e^{-i\eta(p^2/2\hbar)} e^{-i(K_1/\hbar)\cos(q)}. \quad (3)$$

Because the cold atoms are actually moving in a flat space rather than a compact angular space, the quantum resonance condition is relevant only if the initial quantum state is prepared in a definite quasi-momentum state. This is certainly within reach of today's experiments. For example, two recent experiments [16] studied directed transport in a KRM on quantum resonance, with a delocalized BEC (with negligible self-interaction) effectively realizing appropriate initial states such as $|m=0\rangle$. Note also that the quantum map U_{DKRM}^r offers a cold-atom realization of a modified kicked-rotor model we recently proposed [19], where the kinetic energy term can take "negative" values.

With the U_{DKRM}^r realized above, we now present one key numerical result of this work. Figure 1 displays the calculated quasi-energy spectrum of U_{DKRM}^r by the standard diagonalization method [10] as a function of $\tilde{\hbar} \equiv \eta\hbar$, for $K_1/\hbar = K_2/\hbar = 1$, compared with that of U_{KHM} as a function of \hbar , for $K/\hbar = L/\hbar = 1$. The map U_{DKRM}^r is seen to generate a beautiful Hofstadter's butterfly. Even more dramatically, the butterfly of U_{DKRM}^r resembles the previously calculated butterfly of KHM [10] to such a degree that the top panel appears to be indistinguishable from the bottom panel in Fig. 1. The generalized fractal dimensions, denoted by D_q , have also been calculated for many system parameters, confirming that the spectrum is indeed a fractal in general [e.g., for $K_1 = K_2 = 1$, $\tilde{\hbar} = 2\pi/(1 + \sigma)$, $\sigma = (\sqrt{5} + 1)/2$, $D_{q=0} \approx 0.5$, same as the result for the KHM for $\hbar = \tilde{\hbar}$, $K = L = 1$]. Similar results have been found for many other system parameters as well, so long as $\hbar = \tilde{\hbar}$, $K_1 = K$, and $K_2 = L$. To confirm a fractal butterfly spectrum experimentally, one may connect the associated characteristics of the quantum diffusion dynamics (e.g., time dependence of the survival probability, the diffusion exponent, etc.) with the spectrum [21] or attempt to reconstruct the spectrum by first reconstructing the time evolving wave function.

Results in Fig. 1 suggest a strong connection between a DKRM under quantum resonance and the KHM. To uncover this connection let us return to Eq. (3) and temporarily treat

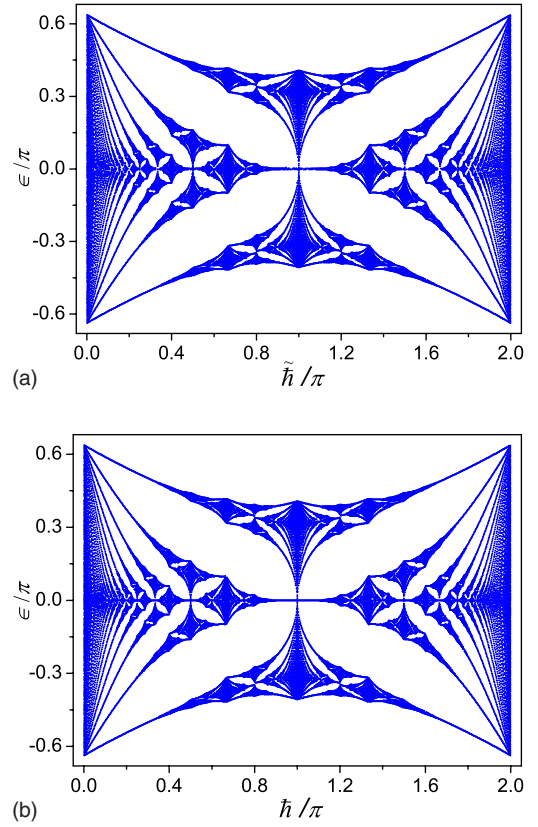


FIG. 1. (Color online) Quasienergy spectrum (denoted ϵ) of the quantum map U_{DKRM}^r given by Eq. (3) (top), compared with that of the KHM map U_{KHM} (bottom) given by Eq. (1). $K_1/\hbar = K_2/\hbar = K/\hbar = L/\hbar = 1$.

it in a flat phase space without the periodic boundary condition. Using the equality $e^{i\eta(p^2/2\hbar)} f(q) e^{-i\eta(p^2/2\hbar)} = f(q + \eta p)$, this treatment leads to

$$U_{\text{DKRM}}^r \rightarrow \tilde{U}_{\text{DKRM}}^r = e^{-i(\tilde{K}_2/\tilde{\hbar})\cos(q+\tilde{p})} e^{-i(\tilde{K}_1/\tilde{\hbar})\cos(q)}, \quad (4)$$

where $\tilde{p} \equiv \eta p$ is a rescaled momentum variable with $[q, \tilde{p}] = i\tilde{\hbar}$, $\tilde{K}_1 = \eta K_1$, and $\tilde{K}_2 = \eta K_2$. Equation (4) now clearly resembles U_{KHM} in Eq. (1), with the only difference being that the first exponential factor of $\tilde{U}_{\text{DKRM}}^r$ in Eq. (4) contains the cos-function of the angle plus the momentum, rather than just the momentum. This already partially rationalizes the strong resemblance between the two panels in Fig. 1.

So is the spectrum of $\tilde{U}_{\text{DKRM}}^r$ identical with that of the KHM? Put differently, does there exist a unitary transformation \mathcal{G} to ensure $\mathcal{G}^\dagger(q + \tilde{p})\mathcal{G} = \tilde{p}$, $\mathcal{G}^\dagger q \mathcal{G} = q$? If such a \mathcal{G} exists, then $\mathcal{G}^\dagger \tilde{U}_{\text{DKRM}}^r \mathcal{G}$ becomes precisely the U_{KHM} in Eq. (1) (with $\tilde{K}_1 \rightarrow K$, $\tilde{K}_2 \rightarrow L$, and $\tilde{\hbar} \rightarrow \hbar$). Significantly, such a \mathcal{G} does not exist for the Hilbert space here. In particular, the above \mathcal{G} transformation is found to assume the analytical form $\mathcal{G} = e^{iq^2/2\tilde{\hbar}}$, which violates the periodic boundary condition associated with $q \rightarrow q + 2\pi$. As such, the spectrum of $\tilde{U}_{\text{DKRM}}^r$, and hence also the spectrum of U_{DKRM}^r in Eq. (3), should contain substantial elements that are absent in the KHM.

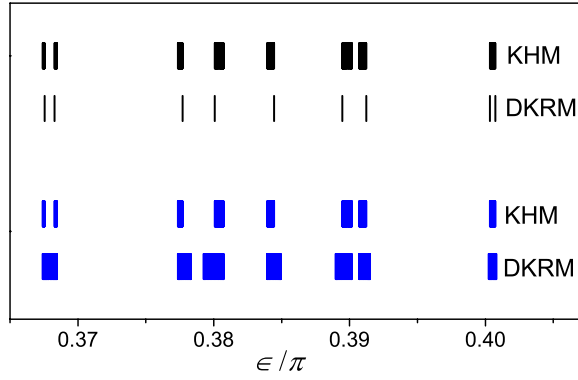


FIG. 2. (Color online) Part of quasienergy spectrum of U_{DKRM}^r in Eq. (3) and U_{KHM} in Eq. (1) for $\hbar = \hbar_0 = 26\pi/41$ (the upper two rows) and $\hbar = \hbar = 2\pi - \hbar_0$ (the lower two rows). $\tilde{K}_1/\tilde{\hbar} = \tilde{K}_2/\tilde{\hbar} = K/\hbar = L/\hbar = 1$. The spectral differences between U_{DKRM}^r and U_{KHM} are evident.

Indeed, as shown in Fig. 2, a more careful comparison does expose spectral differences between U_{DKRM}^r and U_{KHM} . Motivated by this observation, we are also able to find some major differences analytically. For example, for fixed L/\hbar and K/\hbar , the spectrum of U_{KHM} is invariant upon a \hbar -change from \hbar_0 to $2\pi - \hbar_0$. Such a symmetry does not exist in the case of U_{DKRM}^r (see Fig. 2). A second example is for the special case of $\hbar = \tilde{\hbar} = 4\pi$. Therein the spectrum range can be easily found, which is $[-(\tilde{K}_1 + \tilde{K}_2)/\tilde{\hbar}, (\tilde{K}_1 + \tilde{K}_2)/\tilde{\hbar}]$ for U_{DKRM}^r and $[-(K+L)/\hbar, (K-L)/\hbar]$ for U_{KHM} (if none of these range boundaries exceeds $\pm\pi$).

More insights emerge if we examine one interesting classical limit of the DKRM, i.e., the $\tilde{\hbar} \rightarrow 0$ limit (by letting $\eta \rightarrow 0$ with fixed \tilde{K}_1 and \tilde{K}_2) while keeping $T\hbar = 4\pi$. Denote (q_l, \tilde{p}_l) as a classical trajectory right before the l th kick in the $\tilde{\hbar} \rightarrow 0$ limit of U_{DKRM}^r . Then one obtains \tilde{p}_{2l+1}

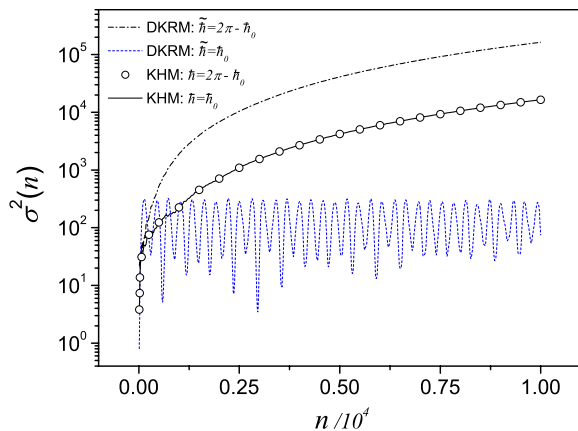


FIG. 3. (Color online) Dynamics of m variance (denoted σ^2) for quantum maps U_{DKRM}^r and U_{KHM} , for the initial state $|0\rangle$. The values of $\hbar = \hbar$ are given by \hbar_0 or $2\pi - \hbar_0$, with $\hbar_0 = 26\pi/41$. $\tilde{K}_1/\tilde{\hbar} = \tilde{K}_2/\tilde{\hbar} = L/\hbar = K/\hbar = 1$. The map U_{KHM} , not U_{DKRM}^r , is seen to be invariant upon the change $\hbar_0 \rightarrow 2\pi - \hbar_0$. Note also that one case associated with U_{DKRM}^r displays localization, and all the others show quadratic diffusion.

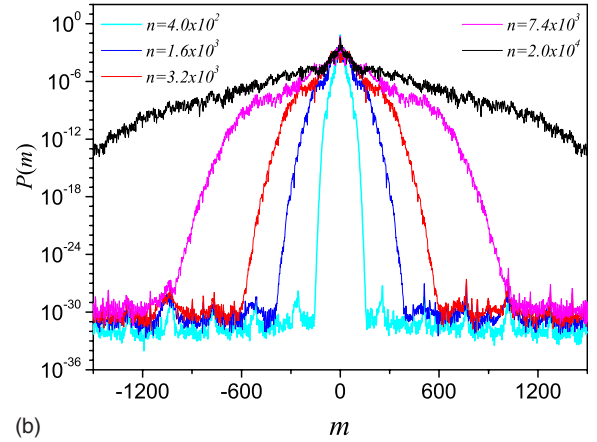
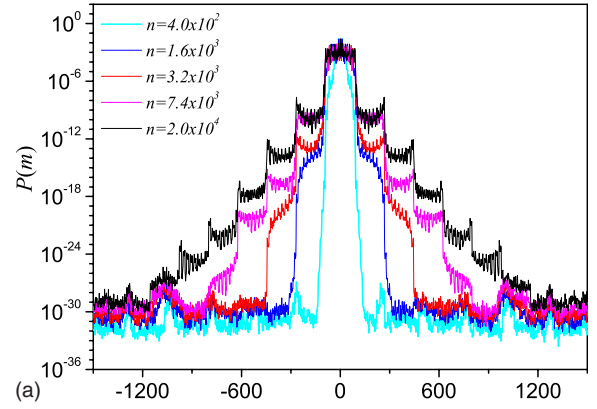


FIG. 4. (Color online) Momentum distribution profile $P(m)$ vs m , evolving from the initial state $|0\rangle$, for U_{DKRM}^r (top) and U_{KHM} (bottom), for $\tilde{\hbar} = \hbar = 2$, $\tilde{K}_1 = \tilde{K}_2 = K = L = 3.7$. In the order of increasing width of the distribution profile, the evolution times are given by $n = 400$, $n = 1600$, $n = 3200$, $n = 7400$, and $n = 20\,000$. The staircase structure seen for U_{DKRM}^r does not exist for U_{KHM} , despite the fact that their two butterfly spectrum is hardly distinguishable.

$= \tilde{p}_{2l} + \tilde{K}_2 \sin(q_{2l})$; $q_{2l+1} = q_{2l} + \tilde{p}_{2l+1}$; $\tilde{p}_{2l+2} = \tilde{p}_{2l+1} + \tilde{K}_1 \sin(q_{2l+1})$; and $q_{2l+2} = q_{2l+1} - \tilde{p}_{2l+2}$. We stress that this classical limit is obtained under quantum resonance, and is hence unrelated to the direct classical analog [22] of the quantum DKRM. Upon making a classical canonical transformation $(q, \tilde{p} + q) \rightarrow (Q, \tilde{P})$, we obtain $\tilde{P}_{2l+2} = \tilde{P}_{2l} + \tilde{K}_2 \sin(Q_{2l})$; $Q_{2l+2} = Q_{2l} - \tilde{K}_1 \sin(\tilde{P}_{2l+2})$, which is precisely the classical map of the kicked Harper model. This finding hence firmly binds the butterfly spectrum of U_{DKRM}^r with the standard KHM. The emergence of the classical KHM map from the $\tilde{\hbar} \rightarrow 0$ limit of U_{DKRM}^r further demonstrates that the spectral differences between U_{DKRM}^r and U_{KHM} arise from genuine quantization effects. Indeed, it is the periodic boundary condition in the quantization that disallows the above mentioned unitary canonical transformation \mathcal{G} as the quantum analog of the classical canonical transformation $(q, \tilde{p} + q) \rightarrow (Q, \tilde{P})$.

The spectral differences between U_{DKRM}^r and U_{KHM} are found to result in profound consequences in the quantum dynamics. One excellent example is shown in Fig. 3, demonstrating clearly that the butterfly associated with U_{DKRM}^r violates a symmetry property of the butterfly associated with

U_{KHM} . Note also that in one case of U_{DKRM}^r shown in Fig. 3, the quantum diffusion displays evident localization that is in clear contrast to the KHM dynamics. This localization behavior suggests that the width of the subbands of the butterfly is effectively zero, in agreement with the result shown as the second row in Fig. 2. Indeed, in our numerical analysis the associated bandwidth is found to be less than 10^{-16} .

To further motivate interests in the new quantum map U_{DKRM}^r we also present in Fig. 4 the time dependence of the momentum distribution profile, for a more generic $\hbar = \tilde{\hbar}$ that is irrational with π . Results therein show again striking differences between U_{DKRM}^r and U_{KHM} , especially in that the former case shows a staircase structure in the profile. Unlike previous observations of analogous staircase structure with a classical origin in an off-resonance DKRM [20], the staircase structure here is purely quantum mechanical. Indeed, both the localization shown in Fig. 3 and the staircase profile shown in Fig. 4(a) can be related to the unique blocked band structure of U_{DKRM}^r in the momentum representation [23]. The important lesson here is that many important features of a quantum map can be hidden in the overall pattern of its butterfly spectrum. For experimental interests, we note that one may tune the value of $\tilde{\hbar}$ and other system parameters to generate different block sizes of U_{DKRM}^r [23], thus attaining staircase steps of less height and hence more accessible to experiments. For example, for $K_1 = K_2 = 14.4$, $\tilde{\hbar} \approx 118\pi/61$,

the associated staircase steps in $P(m)$ have a width of 61, and a height 2–3 orders of magnitude smaller.

Cold-atom realizations of the nonkicked Harper model using static optical lattices were proposed before [24]. However, due to the deep lattice approximation therein they cannot be extended for the kicked Harper model. Based on already available experimental techniques that can achieve a double-kicked rotor model tuned on quantum resonance, here we have proposed a rather simple cold-atom realization of a variant of the kicked Harper model. The results should open up a new generation of cold-atom experiments on quantum maps with a butterfly spectrum. This work also establishes, for the first time, a direct connection between the kicked-rotor model and the kicked Harper model, arguably the two most important paradigms of classical and quantum chaos.

Very constructive comments made by Zai-Qiao Bai are gratefully acknowledged. We thank Shmuel Fishman for insightful comments. We also thank C.-H. Lai for his support and encouragement. J.W. acknowledges support from Defence Science and Technology Agency (DSTA) of Singapore under agreement of POD0613356. J.G. is supported by the start-up funding (WBS Grants No. R-144-050-193-101 and No. R-144-050-193-133) and the NUS ‘‘YIA’’ funding (WBS Grant No. R-144-000-195-123), National University of Singapore.

-
- [1] P. G. Harper, Proc. Phys. Soc., London, Sect. A **68**, 874 (1955).
- [2] D. R. Hofstadter, Phys. Rev. B **14**, 2239 (1976).
- [3] D. Langbein, Phys. Rev. **180**, 633 (1969).
- [4] C. Albrecht *et al.*, Phys. Rev. Lett. **86**, 147 (2001); M. C. Geisler *et al.*, *ibid.* **92**, 256801 (2004).
- [5] Y. Hasegawa and M. Kohmoto, Phys. Rev. B **74**, 155415 (2006).
- [6] D. J. Thouless, Phys. Rev. B **28**, 4272 (1983).
- [7] For example, T. Domanski, M. M. Maška, and M. Mierzejewski, Phys. Rev. B **67**, 134507 (2003).
- [8] For example, Y.-F. Wang, and C.-D. Gong, Phys. Rev. B **74**, 193301(R) (2006); and references therein.
- [9] U. Kuhl and H.-J. Stöckmann, Phys. Rev. Lett. **80**, 3232 (1998).
- [10] T. Geisel, R. Ketzmerick, and G. Petschel, Phys. Rev. Lett. **67**, 3635 (1991); R. Lima and D. Shepelyansky, *ibid.* **67**, 1377 (1991); R. Artuso *et al.*, *ibid.* **69**, 3302 (1992); R. Ketzmerick, K. Kruse, and T. Geisel, *ibid.* **80**, 137 (1998); I. I. Satija, Phys. Rev. E **66**, 015202 (2002); J. B. Gong and P. Brumer, Phys. Rev. Lett. **97**, 240602 (2006).
- [11] A. Iomin and S. Fishman, Phys. Rev. Lett. **81**, 1921 (1998).
- [12] I. Dana, Phys. Lett. A **197**, 413 (1995).
- [13] I. Dana, Phys. Rev. Lett. **73**, 1609 (1994).
- [14] F. L. Moore *et al.*, Phys. Rev. Lett. **75**, 4598 (1995) H. Ammann *et al.*, *ibid.* **80**, 4111 (1998); J. Ringot *et al.*, *ibid.* **85**, 2741 (2000); M. B. d’Arcy *et al.*, *ibid.* **87**, 074102 (2001); G. Duffy *et al.*, Phys. Rev. E **70**, 056206 (2004); H. Lignier *et al.*, Phys. Rev. Lett. **95**, 234101 (2005); P. H. Jones *et al.*, *ibid.* **98**, 073002 (2007); J. F. Kanem *et al.*, *ibid.* **98**, 083004 (2007); J. Chabé *et al.*, e-print arXiv:0709.4320.
- [15] C. Ryu *et al.*, Phys. Rev. Lett. **96**, 160403 (2006).
- [16] M. Sadgrove *et al.*, Phys. Rev. Lett. **99**, 043002 (2007); I. Dana *et al.*, Phys. Rev. Lett. **100**, 024103 (2008).
- [17] P. H. Jones *et al.*, Phys. Rev. Lett. **93**, 223002 (2004).
- [18] G. Casati and B. V. Chirikov, *Quantum Chaos: Between Order and Disorder* (Cambridge University Press, New York, 1995).
- [19] J. B. Gong and J. Wang, Phys. Rev. E **76**, 036217 (2007).
- [20] C. E. Creffield, G. Hur, and T. S. Monteiro, Phys. Rev. Lett. **96**, 024103 (2006); C. E. Creffield, S. Fishman, and T. S. Monteiro, Phys. Rev. E **73**, 066202 (2006); G. C. Carlo *et al.*, Phys. Rev. A **74**, 033617 (2006).
- [21] R. Artuso, G. Casati, and D. Shepelyansky, Phys. Rev. Lett. **68**, 3826 (1992); I. Guarneri and G. Mantica, *ibid.* **73**, 3379 (1994); R. Ketzmerick *et al.*, *ibid.* **79**, 1959 (1997); F. Piéchon, *ibid.* **76**, 4372 (1996).
- [22] L. Cavallasca, R. Artuso, and G. Casati, Phys. Rev. E **75**, 066213 (2007).
- [23] For small $K_1/\hbar = K_2/\hbar$, we analytically find $\langle m | U_{\text{DKRM}}^r | m + 1 \rangle \propto \{1 + \exp[-i\tilde{\hbar}(2m+1)]/2\}$ [19], which can be zero. Hence, to a good approximation this matrix is blocked, especially for $\tilde{\hbar} = 2\pi(2k+1)/(2n+1)$, k, n being integers.
- [24] K. Drese and M. Holthaus, Phys. Rev. Lett. **78**, 2932 (1997); K. Osterloh *et al.*, Phys. Rev. Lett. **95**, 010403 (2005).